NASA TECHNICAL NOTE

NASA TN D-6989

NASA TN D-6989

MULTIMATERIAL LAMINATION AS A MEANS OF RETARDING PENETRATION AND SPALLATION FAILURES IN PLATES

by John D. DiBattista and Donald H. Humes

Langley Research Center
Hampton, Va. 23365

NATIONAL AERONAUTICS AND SPACE ADMINISTRATION • WASHINGTON, D. C. • NOVEMBER 1972

1. Report No.	2. Government Accession No.	3. Recipient's Catalog No.
NASA TN D-6989		

4. Title and Subtitle	5. Report Date
MULTIMATERIAL LAMINATION AS A MEANS OF RETARDING PENETRATION AND SPALLATION FAILURES IN PLATES	November 1972
	6. Performing Organization Code
7. Author(s)	8. Performing Organization Report No.
John D. DiBattista and Donald H. Humes	L-8444
	10. Work Unit No.
9. Performing Organization Name and Address	502-21-29-01
NASA Langley Research Center Hampton, Va. 23365	11. Contract or Grant No.
	13. Type of Report and Period Covered
12. Sponsoring Agency Name and Address	Technical Note
National Aeronautics and Space Administration Washington, D.C. 20546	14. Sponsoring Agency Code

15. Supplementary Notes

16. Abstract This paper presents experimental data which show that hypervelocity impact spallation and penetration failures of a single solid aluminum plate and of a solid aluminum plate spaced a distance behind a Whipple meteor bumper may be retarded by replacing the solid aluminum plate with a laminated plate.

Four sets of experiments were conducted. The first set of experiments was conducted with projectile mass and velocity held constant and with polycarbonate cylinders impacted into single plates of different construction. The second set of experiments was done with single plates of various construction and aluminum spherical projectiles of similar mass but different velocities. These two experiments showed that a laminated plate of aluminum and polycarbonate or aluminum and methyl methacrylate could prevent spallation and penetration failures with a lower areal density than either an all-aluminum laminated plate or a solid aluminum plate. The aluminum laminated plate was in turn superior to the solid aluminum plate in resisting spallation and penetration failures. In addition, through an example of 6061-T6 aluminum and methyl methacrylate, it is shown that a laminated structure ballistically superior to its parent materials may be built.

The last two sets of experiments were conducted using bumper-protected main walls of solid aluminum and of laminated aluminum and polycarbonate. Again, under hypervelocity impact conditions, the laminated main walls were superior to the solid aluminum main walls in retarding spallation and penetration failures.

17. Key Words (Suggested by Author(s))	18. Distribution Statement
Meteor bumper Hypervelocity impact Penetration failure Spallation failure Lamination Meteoroids	Unclassified – Unlimited

19. Security Classif. (of this report)	20. Security Classif. (of this page)	21. No. of Pages	22. Price*
Unclassified	Unclassified	35	$3.00

*For sale by the National Technical Information Service, Springfield, Virginia 22151

MULTIMATERIAL LAMINATION AS A MEANS OF RETARDING PENETRATION AND SPALLATION FAILURES IN PLATES

By John D. DiBattista and Donald H. Humes
Langley Research Center

SUMMARY

This paper presents experimental data which show that hypervelocity impact spallation and penetration failures of a single solid aluminum plate and of a solid aluminum plate spaced a distance behind a Whipple meteor bumper may be retarded by replacing the solid aluminum plate with a laminated plate.

Four sets of experiments were conducted. The first set of experiments was conducted with projectile mass and velocity held constant and with polycarbonate cylinders impacted into single plates of different construction. The second set of experiments was done with single plates of various construction and aluminum spherical projectiles of similar mass but different velocities. These two experiments showed that a laminated plate of aluminum and polycarbonate or aluminum and methyl methacrylate could prevent spallation and penetration failures with a lower areal density than either an all-aluminum laminated plate or a solid aluminum plate. The aluminum laminated plate was in turn superior to the solid aluminum plate in resisting spallation and penetration failures. In addition, through an example of 6061-T6 aluminum and methyl methacrylate, it is shown that a laminated structure ballistically superior to its parent materials may be built.

The last two sets of experiments were conducted using bumper-protected main walls of solid aluminum and of laminated aluminum and polycarbonate. Again, under hypervelocity impact conditions, the laminated main walls were superior to the solid aluminum main walls in retarding spallation and penetration failures.

INTRODUCTION

Large spacecraft, such as space shuttle and space tug which are to be used on many missions, and other spacecraft, such as earth orbiting space stations, lunar exploration vehicles, and, later, manned interplanetary spacecraft which are to be used on long duration missions, will have extremely large area-time product exposures to the meteoroid environment. Because of these large area-time product exposures, the spacecraft will quite likely be impacted by relatively large meteoroids which will have great penetration capability.

Providing adequate protection for the crew and vital equipment against such meteoroids, without severe spacecraft weight penalties, will require careful attention to the spacecraft wall design. In addition to providing meteoroid protection, spacecraft walls must also provide radiation protection, act as a pressure vessel, serve as a load carrying structure, and possibly meet other special mission requirements. The development of the most effective wall to meet all the requirements for a particular mission will become quite complex. Designers of almost all future large spacecraft now plan to use multiplate walls for meteoroid protection. These multiplate walls usually consist of a thin plate (Whipple meteor bumper, ref. 1) spaced a distance in front of a thicker main plate. Such walls are estimated (ref. 2) to be possibly six times as effective as a single-plate wall in providing meteoroid penetration protection. The present paper presents another wall-design consideration involving multimaterial wall construction, which may further increase the meteoroid protection provided by a spacecraft wall without increasing the wall weight.

When multiplate or single-plate metal walls fail from hypervelocity impact, in many instances the first mode of failure encountered is spallation. In situations where sensitive, easily damaged equipment is mounted behind the wall, spalled fragments from the wall can cause considerable damage. If the impact is more severe, the spacecraft wall will suffer a complete penetration and will no longer maintain a pressure differential.

Previous research (refs. 3 to 5) has indicated that a single laminated plate can be made more resistant to spallation and penetration failures than an equal-areal-density solid plate. Tests presented here show that the use of a laminated plate instead of a solid metal plate, both alone and as the main wall of a multiplate structure, will greatly improve the spallation and penetration resistance of the structure. In addition, it is shown that through lamination it is possible to build a structure which is ballistically superior (i.e., better resists spallation and penetration failures) to either of its parent materials.

The physical reasons for the improvement in spallation and penetration resistance offered by laminated walls and a description of four different types of impact tests on such walls are presented herein.

EXPERIMENTAL RESULTS AND DISCUSSION

Physics of Spallation and Penetration Failures in Plates

Single solid plates.- When a hypervelocity projectile impacts a plate, energy is rapidly delivered to the plate from the projectile. This rapid transfer of energy is accomplished by the propagation of shock waves into the plate and into the projectile from the plate-projectile interface (ref. 6). These shock waves both compress and set in

motion the plate as well as compress and slow the projectile. Figure 1(a) illustrates the conditions present in a right circular cylindrical projectile and a plate immediately after impact. The shock waves in the plate and projectile are shown propagating out from the projectile-plate interface. Along with these two shock waves there is a relaxation wave which originates at the circumference of the projectile-plate interface. This relaxation wave acts to release the compressed material behind the shock front and attenuate the shock-wave intensity. After a sufficient amount of time the entire shock front in the plate is affected by this relaxation wave and also by one which originates when the projectile shock wave reaches the projectile rear surface. At a much later time after the impact, the situation present in the plate is as depicted in figure 1(b). The crater being formed in the plate is shown along with the front of the shock wave which has decayed appreciably from its original strength.

Figure 1(c) depicts the situation after the shock or compression wave has reached the plate rear surface and a relaxation wave has begun to propagate back into the plate material. The action of the relaxation waves from the projectile boundaries and the plate rear surface induces a velocity gradient through the plate. The velocity gradient is such that material velocity increases from the crater bottom to the plate rear surface. This leads to a displacement gradient in the plate material. If the displacement gradient becomes large enough, small cracks will form and coalesce, thereby forming a large, rough penny-shaped crack parallel to the plate rear surface as shown in figure 2(a).

The creation of this penny-shaped crack in the plate creates what is called an attached spall (i.e., material between penny crack and rear of plate). Along with the formation of this spall a large amount of kinetic energy is trapped in the spall. If the kinetic energy trapped in the spall disk can be dissipated through plastic-material deformation such that cracks are not produced through the disk from the roughened surface or at the circumference marked "A" and "B" (fig. 2(a)), the spall will not break open or detach from the plate. However, it can be seen that the roughened spall surface and the rigid attachment at A and B are fertile areas for further crack formation.

For more severe impacts, multiple detached spalls may be formed and cracks may propagate in the plate from the last roughened spall surface to the crater bottom. The plate then can no longer hold a pressure differential and will have suffered a penetration failure.

Single laminated plates.- The hypervelocity impact into a similar-material laminated plate proceeds in a similar manner as the hypervelocity impact into a solid plate up to the point where the compression wave reaches the plate rear surface. Figure 2(b) shows the situation at a time after the shock wave has reached the plate rear surface. A relaxation wave from the plate rear surface has reached into the second lamina from the plate rear surface. Because of the velocity gradient, positive from the base of the crater to the plate

rear surface, the individual lamina tends to separate immediately upon arrival of the rear surface relaxation wave at each lamina interface, as shown in figure 2(b). Along with the separation, each lamina traps a decreasing amount of kinetic energy from the plate rear surface toward the crater bottom. The subsequent deflection of each lamina has no influence on a succeeding lamina except to provide the succeeding lamina with an unloaded boundary. Each lamina acts alone to dissipate its trapped kinetic energy through plastic deformation. Here each lamina acts as a smooth sided plate under no rigid constraints. There are, in contrast to figure 2(a), no rough sides and no sharp corners at which cracks may start.

In addition to controlling spallation failures in plates, the use of lamination can also inhibit the formation of penetration failures in plates. As noted previously, the solid plate in figure 2(a) has a roughened area where the spall was formed. Cracks may begin there and propagate through solid material to the crater bottom as the plate deforms to dissipate the kinetic energy it contains. However, in a laminated plate at each lamina interface, any crack formed in a previous lamina must reform on the next lamina which presents a smooth surface for the start of crack formation. The smooth lamina surface makes any crack propagation through the plate extremely difficult. The lack of constraints and roughened surfaces enables a laminated plate to survive a hypervelocity impact without a spallation or penetration failure better than a solid plate.

It appears that an additional improvement in inhibiting spallation and penetration failures is possible with the laminated-plate concept if the compression wave passing into the rear laminae can be attenuated. Such a change in the compression wave profile can be effected by inserting a lamina of lower density than the surrounding laminae. By effecting a decrease in the compression-wave intensity, succeeding laminae are subjected to gentler acceleration from the compression and relaxation waves and their chance of survival is enhanced.

Bumper-protected plates.- The spall and penetration phenomena just discussed for a solid or laminated plate are also valid for the main wall of a meteoroid-bumper main-wall system if the meteoroid and meteoroid-bumper collision results in a spray cloud of large dispersed fragments. In this case each fragment acts individually as it impacts the main wall.

Another case of interest in the meteoroid-bumper main-wall operation is the concerted action of a large number of small individual particles impacting close together on the main wall. Here very little main-wall material is needed to stop the small particles, but a large planar compression wave is driven into the main wall. The reaction of the main wall to a broad flat intensive compression loading would be similar to that of a plate impacted by a single particle, and efforts which improve the latter to resist spallation and penetration failure would improve the former.

Experimental Evaluation of Solid and Laminated Plates

Test setup.- A 220 Swift rifle was used to accelerate projectiles in the velocity range of 1.8 km/sec to 2.2 km/sec. For projectile velocities between 2.2 and 3.9 km/sec, a light-gas gun previously described in reference 7 was used. Each projectile was detected and photographed at two reflected light projectile stations 0.914 meter apart. The time between photographs was divided into the distance traveled by the projectile to calculate the projectile velocity.

A light-gas gun similar to that described by Curtis in reference 8 was used to accelerate projectiles to velocities greater than 3.9 km/sec. The projectile was detected when it interrupted each of two laser beams 10 cm apart, and the time between interruptions was recorded to establish the projectile velocity. The projectiles were also photographed with a six-frame image converter camera. Dividing the distance the projectile traveled between photographs by the time between photographs yielded a projectile velocity within 3 percent to that calculated using the interrupted laser-beam system (ref. 9). All impacts were normal to the plate.

Projectiles and plates.- Both cylindrical and spherical projectiles were used in the experiments. The cylinders of aspect ratio 1 having masses between 160 and 168 mg were made of polycarbonate (1.2 g/cm^3) and were launched at velocities between 6.4 and 7.05 km/sec. The spheres made of 2017-T4 aluminum had masses between 5.8 and 47.2 mg and were launched at velocities between 0.84 and 8.09 km/sec.

The plate configurations used in the experiments were single solid or laminated plates and two spaced plates, with the first plate always solid and the second plate either solid or laminated. Materials used in the plates were 6061-T6 and 2024-T3 aluminum, methyl methacrylate, and polycarbonate. The particular configuration used in each experiment is listed in tables I to IV.

A penetration failure is defined to be the case where a dye penetrate was able to travel through the plate with a 1 atmosphere pressure differential. A spallation failure is defined to be the case where material detaches from the plate rear surface and a dye penetrate was not able to travel through the plate with a 1 atmosphere pressure differential.

Impacts Into Single Solid and Laminated Plates With Polycarbonate Projectiles

From table I, shots 1 and 2 were impacts conducted into solid plates of 6061-T6 aluminum. The front and rear surface of a solid 1.905-cm-thick plate, shot 1, is shown in figure 3. The front and rear surface of a solid 1.50-cm-thick plate, shot 2, is shown in figure 4. The 1.905-cm-thick plate has a multiple spall failure at its rear surface.

The spalls can be seen still attached to the plate. The 1.50-cm-thick plate has suffered spall detachment and a penetration failure.

Shots 3, 4, and 5 were fired to determine if a laminated plate made up of 6061-T6 aluminum would be less susceptible to spallation and penetration failures. Shot 3 was with a target composed of 11 lamina of 6061-T6 aluminum each 0.170 cm thick and having nearly the same areal density as shot 1. No spallation failure occurred. Figure 5 is a side view of the target. Although it cannot be seen in this side view, the successive final deflections of the laminae at the impact axis do not match. The gap between successive laminae increases in passing from the first lamina to the last lamina, indicating that the kinetic energy dissipated in each lamina increased. Shot 4 was with a target composed of nine 6061-T6 aluminum laminae each 0.167 cm thick and having nearly the same areal density as shot 2. Figure 6 shows a side view of the impacted target. No penetration failure or spallation failure has occurred even though shot 4 was with a plate having an areal density less than that of shot 1 and similar to that of shot 2. Shot 5 was with a target composed of seven 6061-T6 aluminum laminae each 0.167 cm thick and having an areal density of 3.16 g/cm^2. This plate shown in figure 7 suffered a spallation and penetration failure.

In order to further reduce the areal density of the plate and still prevent penetration and spallation failures, a multimaterial laminated plate was constructed. Shots 6 and 7 were with these multimaterial laminated plates. Shot 6 was with a plate composed of five 6061-T6 aluminum laminae each 0.167 cm thick, followed by two polycarbonate laminae each 0.254 cm thick, followed by a 6061-T6 aluminum lamina 0.167 cm thick. Photographs of each lamina of the laminated plate are shown in figure 8. The areal density of this laminated plate is similar to that of shot 5. Although the 6061-T6 laminated plate in shot 5 failed, the multimaterial laminated plate of shot 6 did not fail.

The last shot, shot 7, used a plate having an areal density of 2.91 g/cm^2 which is less than any of the previous plates. Its construction was similar to shot 6 except that it had only four 0.170-cm-thick laminae of 6061-T6 aluminum in front. Figure 9 shows the damage done to this target. It has not failed in any way. In these experiments the laminated plate of 6061-T6 aluminum and polycarbonate was a more effective barrier than the aluminum laminated plate or the solid aluminum plate, and the aluminum laminated plate was in turn a more effective barrier than the solid aluminum plate.

Impacts Into Single Solid and Laminated Plates With Aluminum Projectiles

The data were taken using 6-mg-mass aluminum spheres and is recorded in table II and plotted in figure 10 which has an ordinate of plate areal density and an abcissa of impact velocity. To order the significance of the test points, consider the tests shots

using the 6-mg-mass aluminum projectiles which were fired into solid plates of 6061-T6 aluminum. It was established that in the velocity range from 6 to 7.25 km/sec spallation and plate penetration failure occurred in plates having areal densities less than 0.135 g/cm^2. These test points were then used as bench marks against which various laminated structures of 6061-T6 aluminum, polycarbonate, and methyl methacrylate were compared. The structures containing polycarbonate or methyl methacrylate are identified in figure 10; and, in general, it can be seen that the laminated plates are superior to the solid metal plates.

To examine the ballistic properties of polycarbonate and methyl methacrylate alone, several shots were made into these structures alone; and these shots are included in the data plotted as shots 7 to 18 from table II. It can be seen that polycarbonate is much superior to 6061-T6 aluminum in resisting spallation and penetration failure. To examine the importance of lamination and the use of multimaterial laminated plates, data from figure 10 in the velocity range from 6.25 to 7.25 km/sec are plotted in figure 11, which has an ordinate of plate areal density (g/cm^2) and an abscissa of percent aluminum and percent polycarbonate. Again, it can be immediately seen that an all-polycarbonate structure is superior to an all-aluminum structure. But also, it can be noted that laminated structures of 6061-T6 aluminum with less than 20 percent polycarbonate are also superior to the solid aluminum plates. Of course, the superior ballistic performance of these laminated plates could be attributed simply and solely to the fact that polycarbonate is superior ballistically to the aluminum it replaces. That this is not so and that a ballistically superior laminated plate may be constructed from two ballistically inferior materials is shown in figure 12. Here, the plates have been constructed from 6061-T6 aluminum and methyl methacrylate alone and the laminated plates, from both. The velocity range again extends from 6.25 to 7.25 km/sec. As can be seen, the laminated plate is superior to the solid 6061-T6 aluminum and solid methyl methacrylate in spallation and penetration failure.

Impacts Into Bumper-Protected Solid and Laminated Main Walls With Aluminum Projectiles of Various Mass and Velocity

Figure 13 shows schematically the spaced plate configurations used for the tests. The first plate, the meteor bumper, was always a 0.042-cm 2024-T3 aluminum plate. The second plate, or main wall spaced 2.54 cm away, was either a solid 0.206-cm 2024-T3 aluminum plate or a multimaterial laminated plate consisting of two 0.042-cm-thick 2024-T3 aluminum laminae, a polycarbonate lamina 0.178 cm thick, and finally a 0.042-cm 2024-T3 aluminum lamina. The mass distribution for these two configurations is approximately 20 percent in the bumper and 80 percent in the main wall. The ratio of the areal density (g/cm^2) of the laminated and solid main wall had a value of approximately 1.

From table III the pertinent data on projectile mass and velocity and plate configuration may be read for each bumper-protected main-wall test. Also, shown is a check mark indicating whether the main wall failed in a penetration failure or had no penetration failure. *Figure 14 is a plot of the data from table III. The ordinate and abscissa of this plot* are labeled with the projectile mass in mg and projectile velocity in km/sec. The impact conditions, that is the projectile mass and velocity at which each structure was tested, are represented by the diamond symbols for the solid main wall and square symbols for the laminated main wall. An open diamond represents impact conditions at which the solid main wall suffered a penetration failure. A closed diamond indicates no such failure. In a parallel manner the open squares represent penetration failures of the laminated main wall and a closed square indicates no failure. A solid curve for the laminated main wall and a dash-dot curve for the solid main wall have been drawn through the data. Impact conditions above each curve represent penetration failure conditions, and impact conditions below each curve represent conditions of no such failure.

An examination of the curves (fig. 14) shows that the solid aluminum main wall is slightly better for impact velocities from 0.84 up to 2.8 km/sec. In this region of projectile velocity the projectile is not fragmented appreciably by the bumper. Both intact projectile and bumper plug at these low velocities can more easily penetrate the laminated main wall than the solid main wall.

At impact velocities slightly below 2.8 km/sec the projectile began being fractured and dispersed by the bumper. This fracturing and dispersing process increased as projectile velocity increased and produces the upturn in the penetration curves. The increased effectiveness of the laminated wall over the solid main wall in withstanding penetration failures is apparent. At 3.6 km/sec the projectile mass required to penetrate the laminated main wall is at least a factor of 2.0 greater than that needed for the solid main wall. The factor continued to be 2.0 to the highest velocities reached in the tests. Several figures have been included to show the final deformed shape of several laminated and solid main walls. Figures 15 and 16 show the failure and no failure of laminated plates with 20-mg projectiles in a velocity range of 3.0 km/sec to 3.9 km/sec. Figures 17 and 18 show failure and no failure of the solid main wall for a 25-mg and 20-mg projectile with velocities in the 6.8 to 7.0 km/sec range. In a similar velocity range extending from 6.2 to 7.1 km/sec, figures 19, 20, and 21 show no failures and failure of laminated main walls from 35-, 40-, and 47-mg projectiles. The petaling type failure shown in figure 21 is very typical of the failures sustained by the laminated plates.

A detailed examination of the solid aluminum main walls shown in figures 17 and 18 shows the brittle material response of the walls to the projectile-bumper debris cloud. It appears that an extremely short duration but intense compression wave was produced in the main wall by the impacting debris cloud. Reflection of a relaxation wave after the

intense compressional wave reached the main-wall rear surface helped induce a large velocity gradient and, therefore, a large displacement gradient normal to the main-wall surfaces over a large circular area in the plate. A large penny-shaped crack formed and a spallation failure occurred, leaving a roughened spall area shown in figures 17 and 18. Then, in shot 30 either stresses in the main-wall material between the spall region and upper pitted surface of the main wall propagated cracks from the roughened spall area through to the pitted main-wall front surface to form a hole in the plate, or another spall formed to leave the hole in the main wall. A lack of control of the activity of the compression and relaxation waves has made the solid aluminum main walls particularly susceptible to failure. On the other hand, a detailed examination of the laminated main walls shows the no-failure results which can be achieved through control of the compression and relaxation waves by varying material properties throughout the plate thickness. Figures 19 and 20 are good examples of the operation of the laminated plate where each lamina has fulfilled its part in preventing laminated-plate failure. The first two metal laminae have stopped the debris of projectile and bumper. The polycarbonate lamina used as a shock-wave attenuator separating the outer aluminum laminae shows slight penetration at the center and large circular cracks at approximately 9 to 12 projectile radius. The last aluminum lamina used to trap the compression pulse and dissipate its energy through plastic deformation is shown in a final bulged condition, but still with no cracks through it. After an examination of these targets it can be noted that the laminated plates used here did not exhibit a separate spallation mode of failure as did the solid main walls (fig. 18). The solid main walls under these impact conditions have spallation failures before sustaining a penetration failure, and therefore a spallation-failure curve would be below the solid main-wall penetration curve in figure 14. Therefore, the superiority of the laminated main wall over the solid main wall is obvious from a spallation point of view also.

Impacts Into Bumper-Protected Main Walls With Aluminum Projectiles Of Similar Mass and Different Velocities

In an effort to examine the behavior of the main wall under impact with highly fragmented projectile and bumper debris clouds, 6-mg spheres of 2017-T4 aluminum were launched to 8.1 km/sec into targets having a 0.043-cm-thick bumper spaced 0.8 cm away from various solid and laminated main walls. From the data tabulated in table IV, figure 22 has been constructed. Under these impact conditions 6061-T6 and 2024-T3 aluminum solid main walls failed in spallation at areal densities around 0.850 g/cm^2 and penetration failures were possible in plates having areal densities less than 0.430 g/cm^2. Compared ballistically with these tests are various two- and three-layer laminated plates. These laminated plates were of areal density less than 0.420 g/cm^2. After an examina-

tion of the data points in figure 22 it can be seen that a laminated plate can be built which is superior to a solid aluminum plate in resisting spallation and penetration failures.

CONCLUSIONS

Four sets of experiments have been conducted to study the effect lamination has on spallation and penetration failures in plates subjected to hypervelocity impacts by single and multiple particles.

The first set of experiments showed that the areal density of a single plate could be reduced by 20 percent through lamination alone and by 40 percent through the use of multimaterial lamination. The second set of experiments showed that multimaterial lamination is an effective means of resisting spallation and penetration failures in a single plate. This second set of experiments exposed the fact that polycarbonate alone is an extremely effective barrier to high-speed particles. In addition, it was shown during these experiments that a laminated structure may be built which is ballistically superior to its parent materials.

The third set of experiments showed that a bumper-protected laminated main wall with the same areal density as a solid main wall could withstand spallation and penetration failure by impacting particles twice as massive as those which penetrated and spalled the solid main wall. The fourth set of experiments was done with bumper-protected solid and laminated main walls. Under conditions where the debris cloud is in a highly fragmented state, it was demonstrated again that a multimaterial laminated main wall is superior to a solid main wall.

Langley Research Center,
National Aeronautics and Space Administration,
Hampton, Va., November 1, 1972.

REFERENCES

1. Whipple, F. L.: Meteorites and Space Travel. Astron. J., vol. 52, Feb. 1947, p. 131.

2. Humes, Donald H.: Calculation of the Penetration Flux for a Multiwall Structure on the Lunar Orbiter Spacecraft. NASA TN D-5455, 1969.

3. McMillan, A. R.: An Investigation of the Penetration of Hypervelocity Projectiles Into Composite Laminates. Proceedings of the Sixth Symposium on Hypervelocity Impact, vol. III (AD 423 802), Aug. 1963, pp. 309-356. (Sponsored by U.S. Army, U.S. Air Force, and U.S. Navy.)

4. Gehring, J. Wm.; Christman, D. R.; and McMillan, A. R.: Hypervelocity Impact Studies Concerning the Meteoroid Hazard to Aerospace Materials and Structures. AIAA Fifth Annual Structures and Materials Conference, Apr. 1964, pp. 78-91.

5. Loeffler, I. J.; Lieblein, Seymour; and Clough, Nestor: Meteoroid Protection for Space Radiators. [Preprint] 2543-62, Amer. Rocket Soc., Sept. 1962.

6. Heyda, J. F.; and Riney, T. D.: Penetration of Structures by Hypervelocity Projectiles. Doc. No. 645D450 (Contract AF 04(694)-222), Re-Entry Syst. Dep., Gen. Elec. Co., Feb. 11, 1964. (Available from DDC as AD 348 439.)

7. Collins, Rufus D., Jr.; and Kinard, William H.: The Dependency of Penetration on the Momentum Per Unit Area of the Impacting Projectile and the Resistance of Materials to Penetration. NASA TN D-238, 1960.

8. Curtis, John S.: An Accelerated Reservoir Light-Gas Gun. NASA TN D-1144, 1962.

9. Kassel, Philip C.; and DiBattista, John D.: An Ultra-High-Speed Photographic System for Investigating Hypervelocity Impact Phenomena. NASA TN D-6128, 1971.

TABLE I

EXPERIMENTAL DATA FOR CYLINDRICAL POLYCARBONATE PROJECTILES IMPACTING SOLID PLATES OF 6061-T6 ALUMINUM, LAMINATED PLATES OF 6061-T6 ALUMINUM, AND LAMINATED PLATES OF 6061-T6 ALUMINUM AND POLYCARBONATE

Shot	Projectile properties				Target properties		Type of failure
	Diameter, cm	Length, cm	Mass, g	Velocity, km/sec	Areal density, g/cm^2	Configuration	
1	0.564	0.553	160	6.94	5.14	Solid aluminum 6061-T6 plate, 1.905 cm thick	Spallation
2	.564	.564	168	6.50	4.05	Solid aluminum 6061-T6 plate, 1.500 cm thick	Spallation and penetration
3	.559	.559	160	7.50	5.05	Eleven aluminum 6061-T6 laminae, each 0.170 cm thick	None
4	.567	.551	161.5	6.40	4.07	Nine aluminum 6061-T6 laminae, each 0.167 cm thick	None
5	.567	.551	162	7.05	3.16	Seven aluminum 6061-T6 laminae, each 0.167 cm thick	Spallation and penetration
6	.567	.551	160.5	7.05	3.31	Five aluminum 6061-T6 laminae, each 0.167 cm thick	None
						Two polycarbonate laminae, each 0.254 cm thick	None
						One aluminum 6061-T6 lamina, 0.167 cm thick	None
7	.567	.551	160.3	6.89	2.91	Four aluminum 6061-T6 laminae, each 0.170 cm thick	None
						Two polycarbonate laminae, each 0.254 cm thick	None
						One aluminum 6061-T6 lamina, 0.167 cm thick	None

TABLE II

EXPERIMENTAL DATA FOR 0.153-cm-DIAMETER SPHERES OF 2017-T4 ALUMINUM IMPACTING SOLID AND LAMINATED PLATES OF 6061-T6 ALUMINUM, METHYL METHACRYLATE, AND POLYCARBONATE

Shot	Target properties																					Total areal density, g/cm^2	Percent aluminum	Percent polycarbonate or methyl methacrylate	Projectile velocity, km/sec	Type of failure
	Lamina 1			Lamina 2			Lamina 3			Lamina 4			Lamina 5			Lamina 6			Lamina 7							
	Thickness, cm	Material	Areal density, g/cm^2	Thickness, cm	Material	Areal density, g/cm^2	Thickness, cm	Material	Areal density, g/cm^2	Thickness, cm	Material	Areal density, g/cm^2	Thickness, cm	Material	Areal density, g/cm^2	Thickness, cm	Material	Areal density, g/cm^2	Thickness, cm	Material	Areal density, g/cm^2					
1	0.488	Al 6061-T6	1.32																			1.32	100	0	6.58	PF
2	.508	↓	1.37																			1.37	100	0	7.21	PF
3	.533	↓	1.44																			1.44	100	0	6.55	PF
4	.559	↓	1.51																			1.51	100	0	6.57	US
5	.635	↓	1.71																			1.71	100	0	6.37	US
6	.081	↓	.218	0.081	Al 6061-T6	0.218	0.081	Al 6061-T6	0.218	0.081	Al 6061-T6	0.218	0.081	Al 6061-T6	0.218							1.09	100	0	6.45	PF
7	0.891	[b]Poly	1.07																			1.07	0	100	7.07	NF
8	.970	↓	1.16																			1.16	0	100	6.97	NF
9	1.29	↓	1.55																			1.55	0	100	6.62	NF
10	.475	↓	.57	0.155	[b]Poly	0.186																.756	0	100	6.63	NF
11	.155	↓	.186	.475	↓	.57																.756	0	100	6.62	NF
12	.617	↓	.74	.155	↓	.186																.926	0	100	6.5	NF
13	0.820	[c]MM	0.975																			0.975	0	100	6.5	PF
14	.889	↓	1.05																			1.05	0	100	6.5	SF
15	.989	↓	1.17																			1.17	0	100	6.6	SF
16	1.016	↓	1.21																			1.21	0	100	6.6	SF
17	1.27	↓	1.51																			1.51	0	100	6.67	SF
18	.635	↓	.755	1.27	[c]MM	1.51																2.26	0	100	6.15	NF
19	0.081	Al 6061-T6	0.218	0.081	Al 6061-T6	0.218	0.063	Al 6061-T6	0.170	0.051	[b]Poly	0.061	0.051	[b]Poly	0.061	0.051	[b]Poly	0.061	0.055	Al 6061-T6	0.149	0.938	81.0	19.0	7.07	PF
20	.081	↓	.218	.081	↓	.218	.063	↓	.170	.051	↓	.061	.051	[b]Poly	.061	.051	[b]Poly	.061	.055	Al 6061-T6	.149	.938	81.0	19.0	6.55	NF
21	.081	↓	.218	.081	↓	.218	.063	↓	.170	.051	↓	.061	.055	Al 6061-T6	.149	.055	Al 6061-T6	.149				.965	93.9	6.1	7.17	PF
22	.081	↓	.218	.081	↓	.218	.081	↓	.218	.102	↓	.122	.081	Al 6061-T6	.218							1.00	88.3	11.7	6.61	NF
23	.320	↓	.865	.076	[b]Poly	.091	.053	↓	.143													1.10	91.9	8.1	6.74	PF
24	.160	↓	.43	.160	Al 6061-T6	.43	.102	[b]Poly	.122	.063	Al 6061-T6	.170										1.15	90.0	10.0	6.50	NF
25	.160	↓	.43	.160	↓	.43	.152	↓	.182	.063	↓	.170										1.212	85.5	14.5	7.11	NF
26	.160	↓	.43	.160	↓	.43	.102	↓	.122	.063	↓	.170	.063	Al 6061-T6	.170							1.32	91.2	8.8	6.79	NF
27	0.051	Al 6061-T6	0.138	0.081	Al 6061-T6	0.218	0.081	Al 6061-T6	0.218	0.150	[c]MM	0.178	0.051	Al 6061-T6	0.138							0.890	81.8	19.2	5.9	PF
28	.160	↓	.43	.053	↓	.143	.155	[c]MM	.184	.053	Al 6061-T6	.143										.900	84.1	15.9	5.95	PF
29	.081	↓	.218	.081	↓	.218	.137	↓	.163	.137	[c]MM	.163	.063	Al 6061-T6	.170							.932	66.0	34.0	5.86	NF
30	.081	↓	.218	.081	↓	.218	.137	↓	.163	.137	↓	.163	.063	↓	.170							.932	66.0	34.0	6.53	NF
31	.081	↓	.218	.081	↓	.218	.147	↓	.175	.147	↓	.175	.063	↓	.170							.956	64.1	35.9	6.48	NF
32	.081	↓	.218	.081	↓	.218	.160	↓	.190	.160	↓	.190	.053	↓	.143							.959	61.0	39.0	6.325	NF
33	.081	↓	.218	.081	↓	.218	.137	↓	.163	.137	↓	.163	.081	↓	.218							.981	67.7	32.2	6.54	NF
34	.081	↓	.218	.081	↓	.218	.180	Al 6061-T6	.218	.132	↓	.157	.081	↓	.218							1.03	85.3	14.7	6.86	NF
35	.081	↓	.218	.081	↓	.218	.081	↓	.218	.132	↓	.157	.081	↓	.218							1.03	85.3	14.7	5.53	NF
36	.081	↓	.218	.150	[c]MM	.178	.081	↓	.218	.081	Al 6061-T6	.218	.081	↓	.218							1.05	83.7	16.3	6.08	NF

[a] PF is penetration failure; US is undetached spallation; NF is no failure; SF is spallation failure.

[b] Poly is polycarbonate.

[c] MM is methyl methacrylate.

TABLE III

EXPERIMENTAL DATA FOR SPHERES OF 2017-T4 ALUMINUM IMPACTING BUMPER-PROTECTED MAIN WALLS OF 2024-T3 ALUMINUM AND LAMINATED MAIN WALLS OF 2024-T3 ALUMINUM AND POLYCARBONATE

Shot	Projectile properties		Main wall configuration (a)	No penetration failure	Penetration failure
	Mass, mg	Velocity, km/sec			
1	6.0	2.82	Figure 13(a)	✓	
2	6.0	3.00	Figure 13(a)	✓	
3	6.0	3.15	Figure 13(a)	✓	
4	6.0	3.50	Figure 13(a)	✓	
5	5.8	6.80	Figure 13(a)	✓	
6	8.3	2.48	Figure 13(a)	✓	
7	8.4	2.96	Figure 13(a)		✓
8	8.4	3.35	Figure 13(a)	✓	
9	8.4	3.48	Figure 13(a)		✓
10	8.7	3.52	Figure 13(a)	✓	
11	8.5	3.67	Figure 13(a)	✓	
12	11.6	1.82	Figure 13(a)	✓	
13	11.0	1.93	Figure 13(a)	✓	
14	11.3	2.14	Figure 13(a)	✓	
15	11.4	2.39	Figure 13(a)		✓
16	11.6	2.85	Figure 13(a)		✓
17	11.6	3.10	Figure 13(a)		✓
18	11.1	3.70	Figure 13(a)		✓
19	11.2	3.93	Figure 13(a)	✓	
20	19.3	1.69	Figure 13(a)	✓	
21	19.7	1.81	Figure 13(a)		✓
22	18.5	3.53	Figure 13(a)		✓
23	20.5	5.69	Figure 13(a)		✓
24	20.5	5.77	Figure 13(a)		✓
25	20.4	6.13	Figure 13(a)	✓	
26	20.3	6.8	Figure 13(a)	✓	
27	20.5	6.84	Figure 13(a)	✓	
28	20.6	7.0	Figure 13(a)	✓	
29	25.0	6.42	Figure 13(a)		✓
30	25.2	6.82	Figure 13(a)		✓
31	31.0	4.5	Figure 13(a)		✓

[a] Areal density of 0.571 g/cm^2.

TABLE III – Concluded

EXPERIMENTAL DATA FOR SPHERES OF 2017-T4 ALUMINUM IMPACTING BUMPER-PROTECTED MAIN WALLS OF 2024-T3 ALUMINUM AND LAMINATED MAIN WALLS OF 2024-T3 ALUMINUM AND POLYCARBONATE

Shot	Projectile properties		Main wall configuration (a)	No penetration failure	Penetration failure
	Mass, mg	Velocity, km/sec			
32	31.0	5.3	Figure 13(a)		✓
33	46.4	1.08	Figure 13(a)	✓	
34	46.4	1.21	Figure 13(a)		✓
35	46.4	2.57	Figure 13(a)		✓
36	46.8	3.10	Figure 13(a)		✓
37	46.4	3.84	Figure 13(a)		✓
38	46.4	5.1	Figure 13(a)		✓
39	46.4	5.6	Figure 13(a)		✓
40	46.4	5.8	Figure 13(a)		✓
41	5.9	1.84	Figure 13(b)	✓	
42	5.9	2.58	Figure 13(b)	✓	
43	11.0	1.43	Figure 13(b)	✓	
44	11.7	1.91	Figure 13(b)		✓
45	11.7	2.45	Figure 13(b)		✓
46	11.4	2.82	Figure 13(b)		✓
47	11.0	3.19	Figure 13(b)	✓	
48	19.3	1.45	Figure 13(b)	✓	
49	20.4	1.52	Figure 13(b)	✓	
50	20.4	1.64	Figure 13(b)		✓
51	19.4	1.86	Figure 13(b)		✓
52	20.4	3.01	Figure 13(b)		✓
53	20.0	3.29	Figure 13(b)		✓
54	20.2	3.88	Figure 13(b)	✓	
55	28.5	6.56	Figure 13(b)	✓	
56	30.1	6.84	Figure 13(b)	✓	
57	35.0	6.81	Figure 13(b)	✓	
58	40.2	7.10	Figure 13(b)	✓	
59	46.9	.84	Figure 13(b)	✓	
60	46.8	.88	Figure 13(b)	✓	
61	46.9	1.21	Figure 13(b)		✓
62	47.2	6.20	Figure 13(b)		✓
63	47.2	7.34	Figure 13(b)		✓

[a] Areal density of 0.571 g/cm^2.

TABLE IV

EXPERIMENTAL DATA FOR 0.157-cm-DIAMETER SPHERES OF 2017-T4 ALUMINUM IMPACTING VARIOUS BUMPER-PROTECTED MAIN WALLS CONTAINING 6061-T6 ALUMINUM, 2024-T3 ALUMINUM, AND POLYCARBONATE[a]

Shot	Symbol	Lamina 1		Lamina 2		Lamina 3		Areal density, g/cm^2	Projectile velocity, km/sec	Type of failure
		Thickness, cm	Material	Thickness, cm	Material	Thickness, cm	Material			
1	○	0.318	Al 2024-T3					0.88	7.94	[b]SF
2	○	.208	Al 2024-T3					.574	7.84	SF
3	○	.162	Al 2024-T3					.449	8.09	[c]PF
4	○	.160	Al 2024-T3					.444	7.75	PF
5	○	.127	Al 2024-T3					.352	7.06	PF
6	▱	.360	Al 6061-T6					.972	6.82	[d]US
7	▱	.330	Al 6061-T6					.891	6.40	SF
8	▱	.318	Al 6061-T6					.859	7.12	SF
9	▱	.234	Al 6061-T6					.631	6.85	SF
10	▱	.160	Al 6061-T6					.432	5.55	PF
11	▱	.160	Al 6061-T6					.432	6.85	SF
12	▭	.127	Polycarbonate	0.051	Al 2024-T3			.293	6.7	[e]NF
13	◇	.152	Polycarbonate	.043	Al 2024-T3	0.043	Al 2024-T3	.420	7.87	NF
14	◇	.101	Polycarbonate	.043	Al 2024-T3	.043	Al 2024-T3	.359	7.58	PF
15	△	.076	Polycarbonate	.051	Al 2024-T3	.043	Al 2024-T3	.351	6.94	PF
16	△	.076	Polycarbonate	.051	Al 2024-T3	.043	Al 2024-T3	.351	6.58	NF
17	△	.076	Polycarbonate	.051	Al 2024-T3	.043	Al 2024-T3	.351	6.30	NF
18	△	.076	Polycarbonate	.051	Al 2024-T3	.043	Al 2024-T3	.351	6.07	NF
19	◇	.076	Polycarbonate	.051	Polycarbonate	.051	Al 2024-T3	.373	6.90	NF
20	◇	.076	Polycarbonate	.051	Polycarbonate	.051	Al 2024-T3	.373	6.68	NF
21	□	.076	Polycarbonate	.043	Al 2024-T3	.043	Al 2024-T3	.329	7.69	PF
22	□	.076	Polycarbonate	.043	Al 2024-T3	.043	Al 2024-T3	.329	7.0	PF
23	□	.076	Polycarbonate	.043	Al 2024-T3	.043	Al 2024-T3	.329	6.73	NF
24	□	.076	Polycarbonate	.043	Al 2024-T3	.043	Al 2024-T3	.329	6.68	NF
25	□	.076	Polycarbonate	.043	Al 2024-T3	.043	Al 2024-T3	.329	6.11	NF
26	⬠	.076	Polycarbonate	.081	Al 2024-T3			.315	6.15	PF
27	◁	.076	Polycarbonate	.048	Al 2024-T3			.224	6.9	PF
28	◁	.076	Polycarbonate	.043	Al 2024-T3	.025	Al 2024-T3	.279	6.79	PF
29	▽	.076	Polycarbonate	.063	Al 6061-T6			.261	6.81	PF
30	▽	.076	Polycarbonate	.063	Al 6061-T6			.261	6.64	PF
31	▽	.076	Polycarbonate	.063	Al 6061-T6			.261	6.44	PF

[a] All bumpers were 0.043-cm-thick 2024-T3 aluminum; all spacings were 0.8 cm.

[b] SF is spallation failure.

[c] PF is penetration failure.

[d] US is undetached spallation.

[e] NF is no failure.

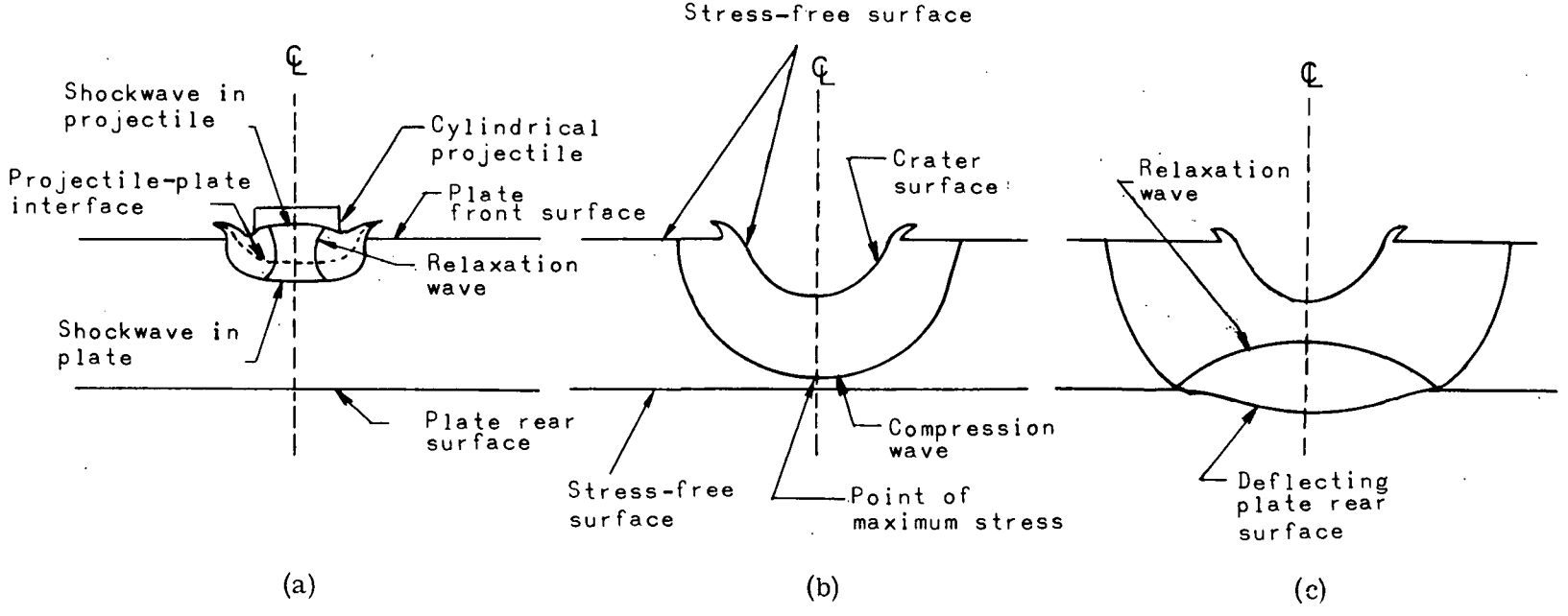

Figure 1.- Side views of a cylindrical projectile penetrating a finite thickness plate at various times after impact.

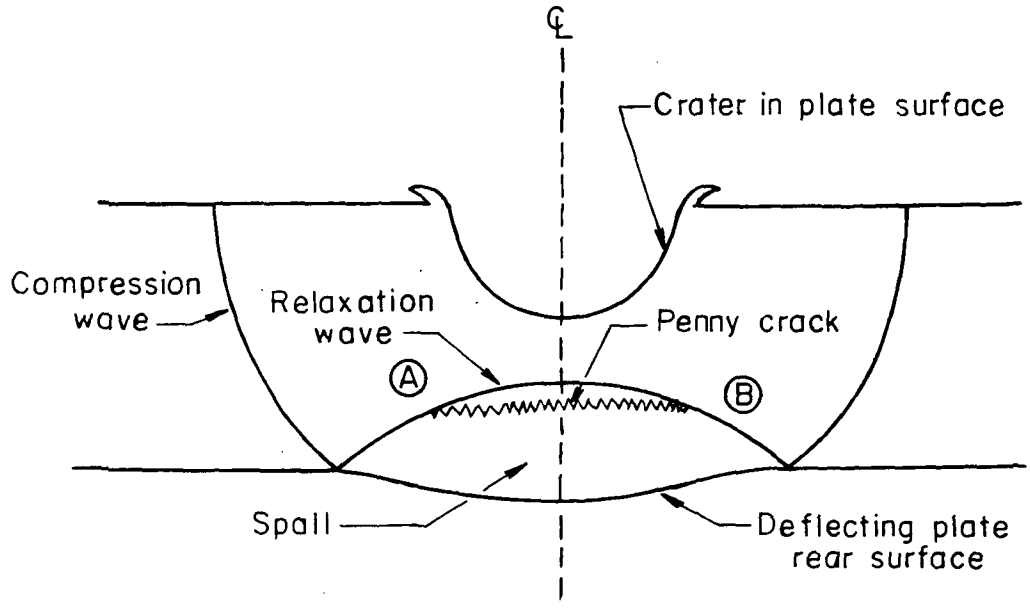

(a)

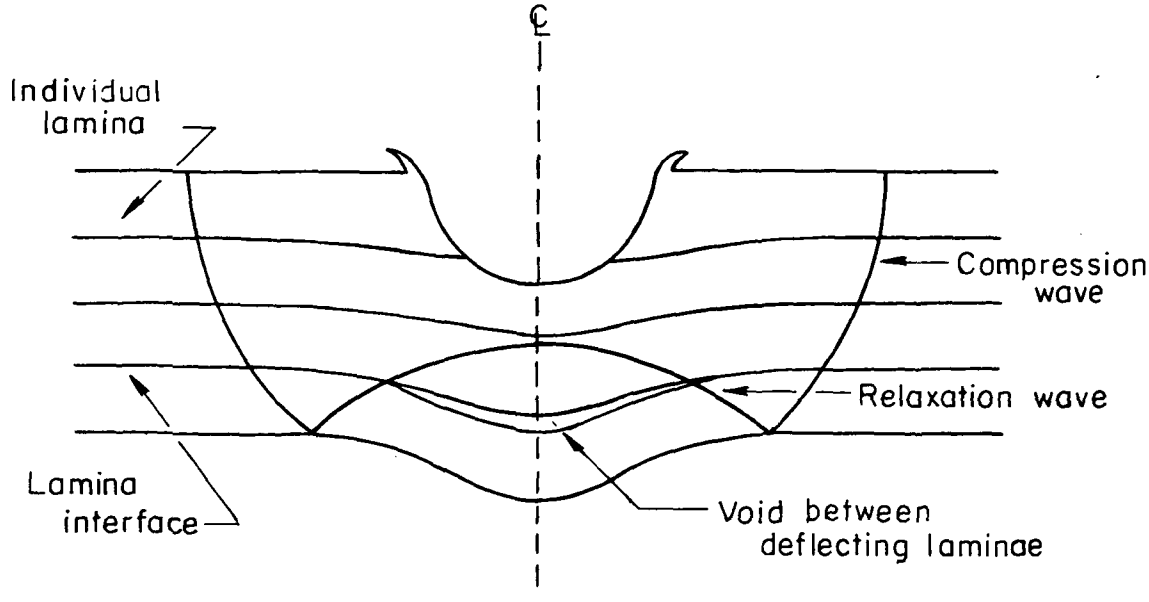

(b)

Figure 2.- Condition present in plate after compression wave reaches plate rear surface.

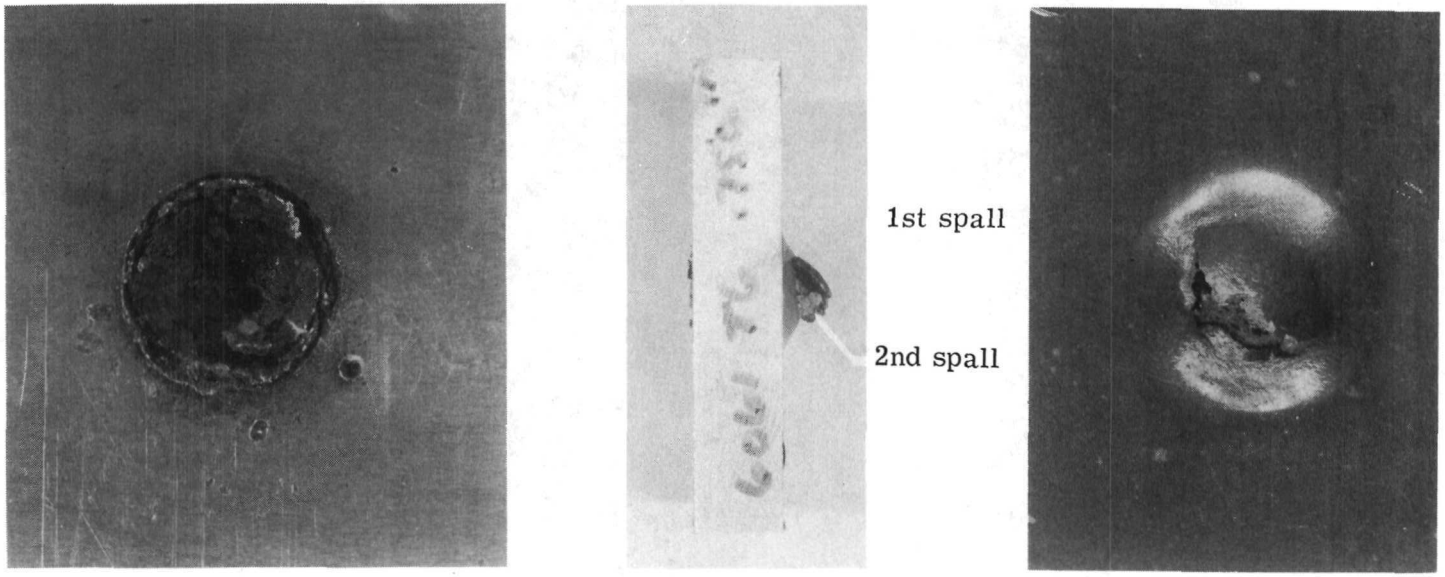

Front view Side view Back view

L-72-6561

Figure 3.- Photographs showing multiple spall failure at the rear surface of plate used in shot 1, table I.

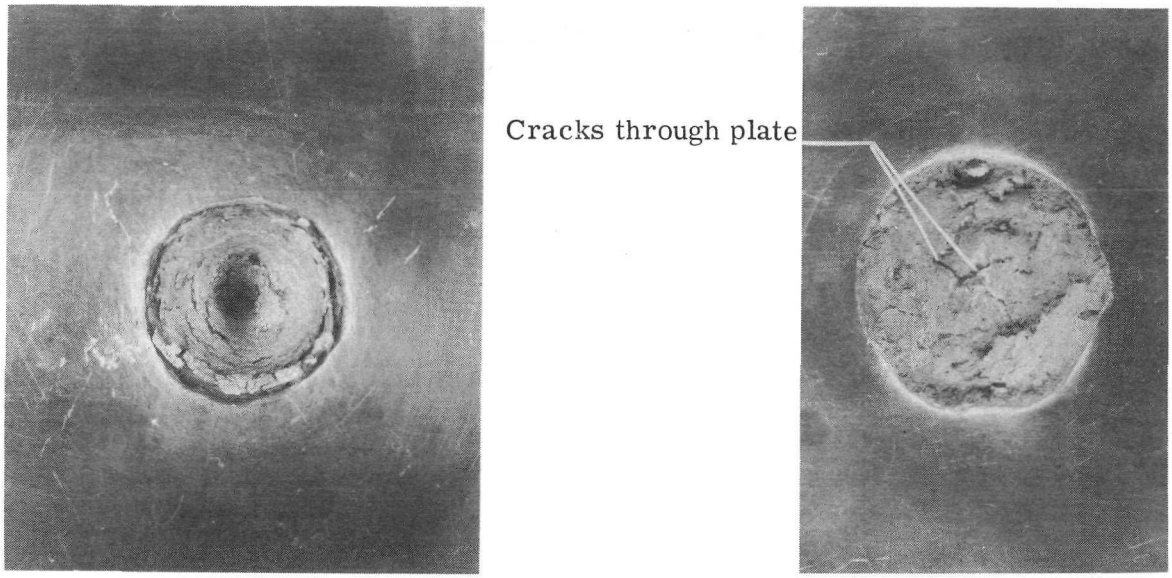

Front view

Back view

L-72-6562

Figure 4.- Photographs showing detached spall and penetration failure of plate used in shot 2, table I.

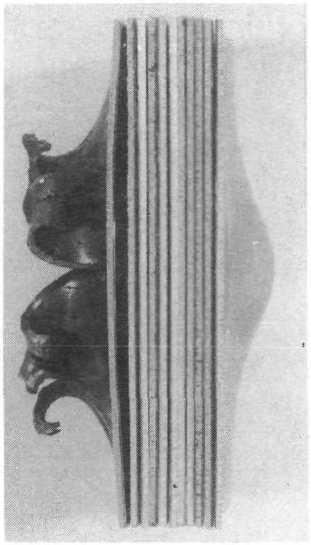

L-72-6563

Figure 5.- Photograph from side of plate used in shot 3, table I.

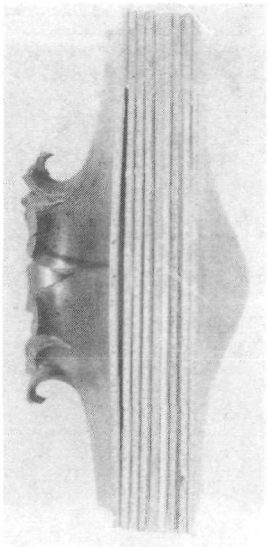

L-62-6564

Figure 6.- Photograph from side of plate used in shot 4, table I.

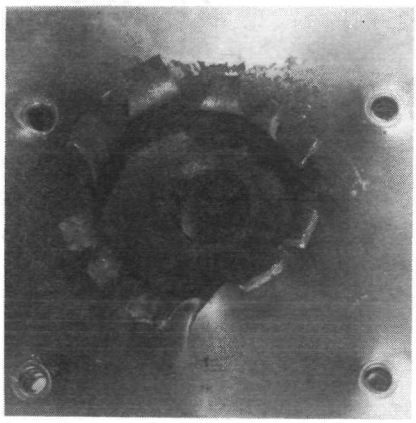

Front view

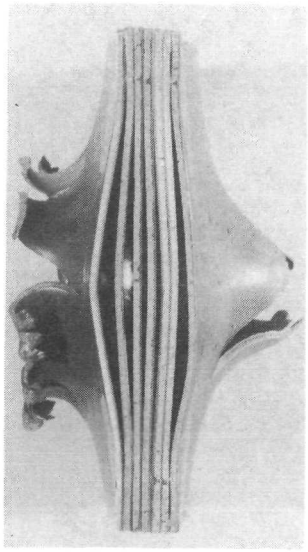

Side view

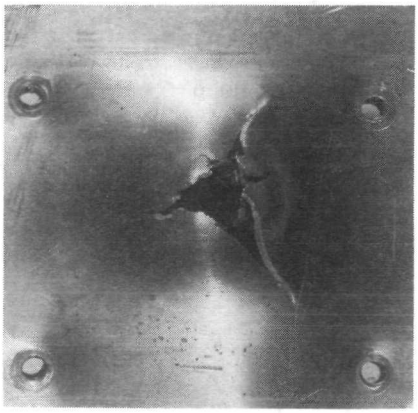

Back view

L-72-6565

Figure 7.- Photographs of damage to plate used in shot 5, table I.

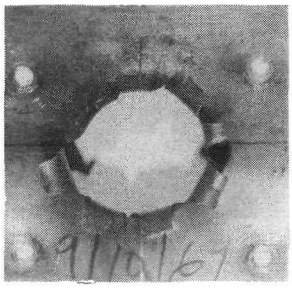

Lamina 1

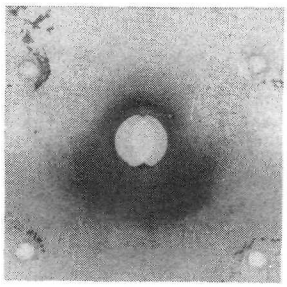

Lamina 2

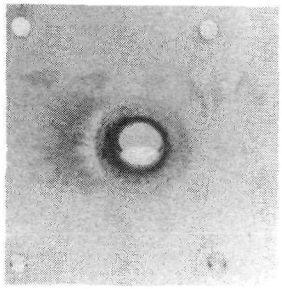

Lamina 3

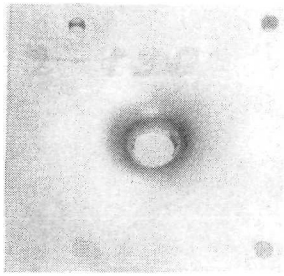

Lamina 4

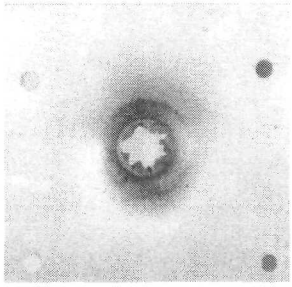

Lamina 5

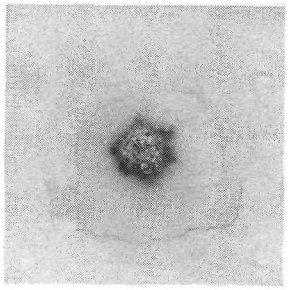

Lamina 6

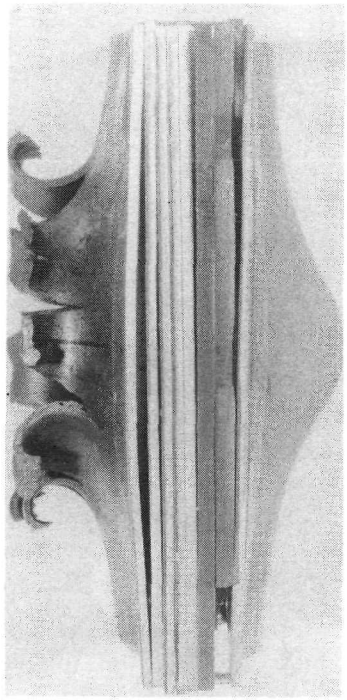

Side view

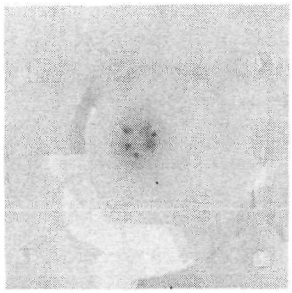

Lamina 7

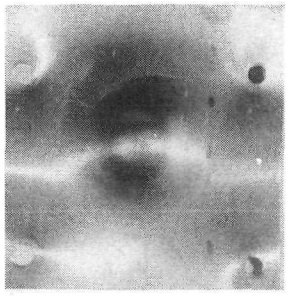

Lamina 8

L-72-6566

Figure 8.- Photographs of damage done to individual laminae used in shot 6, table I.

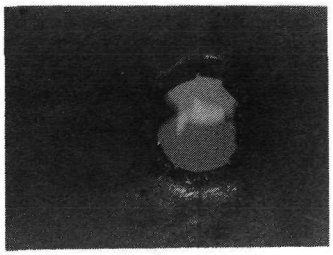

Lamina 1

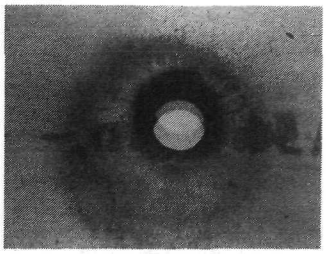

Lamina 2

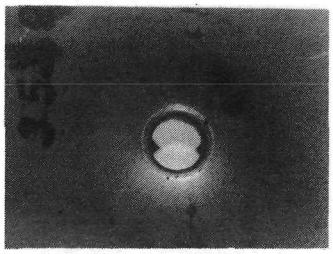

Lamina 3

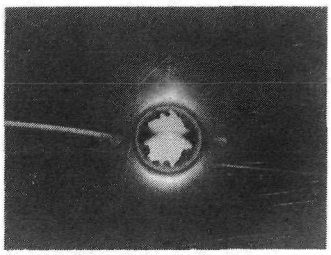

Lamina 4

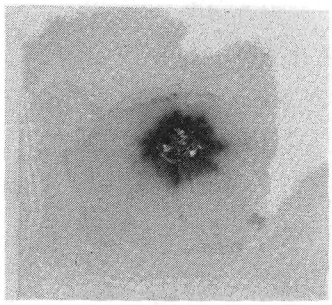

Laminae 5 and 6

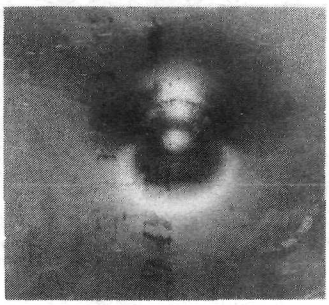

Lamina 7

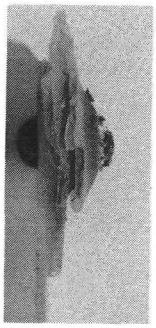

Side view, laminae 5 and 6

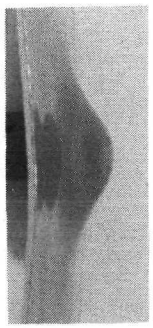

Side view, lamina 7

L-72-6567

Figure 9.- Photographs of damage done to individual laminae of plate used in shot 7, table I.

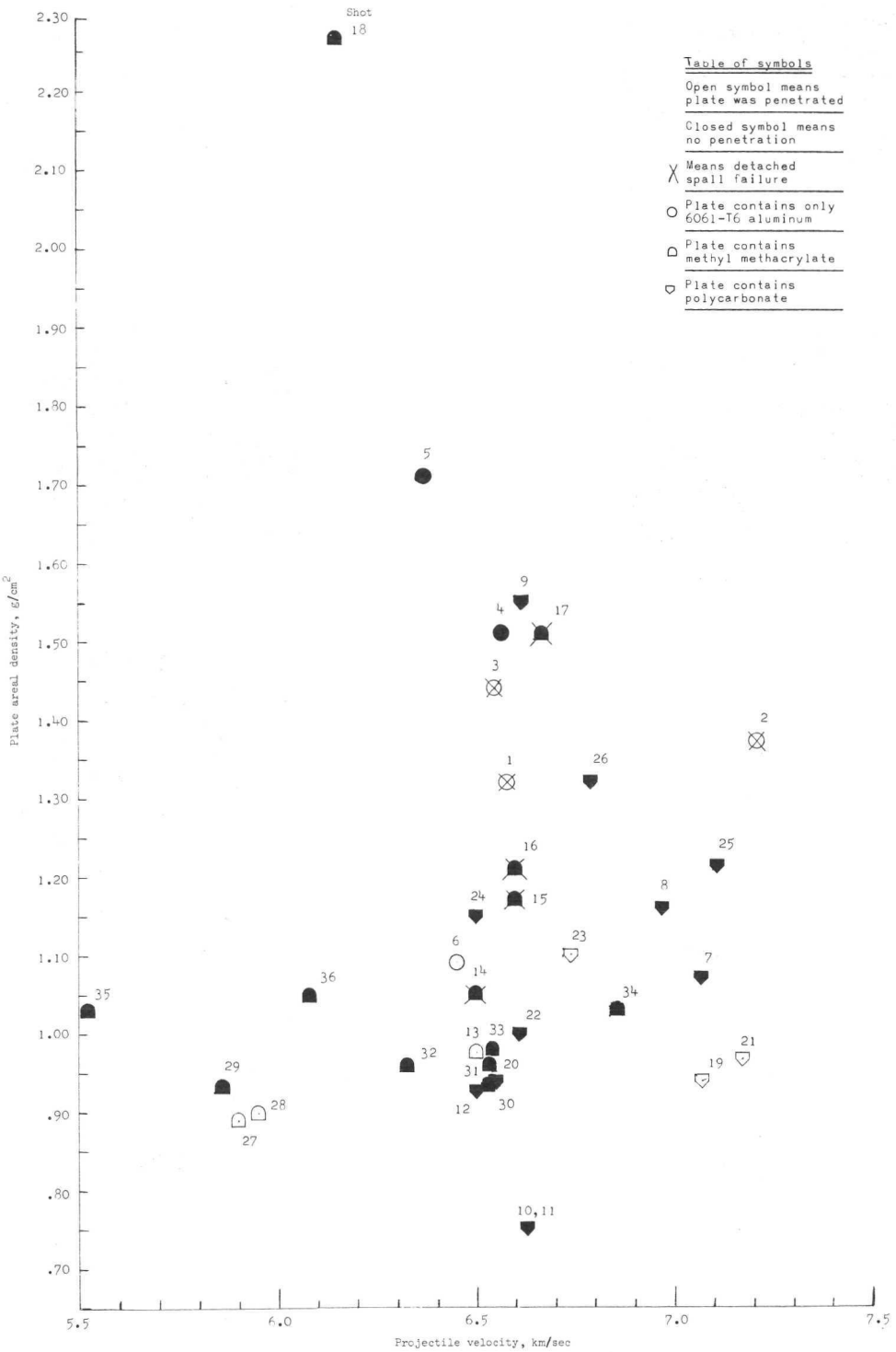

Figure 10.- Penetration data from table II for various single plates impacted by 0.153-cm-diameter aluminum spheres.

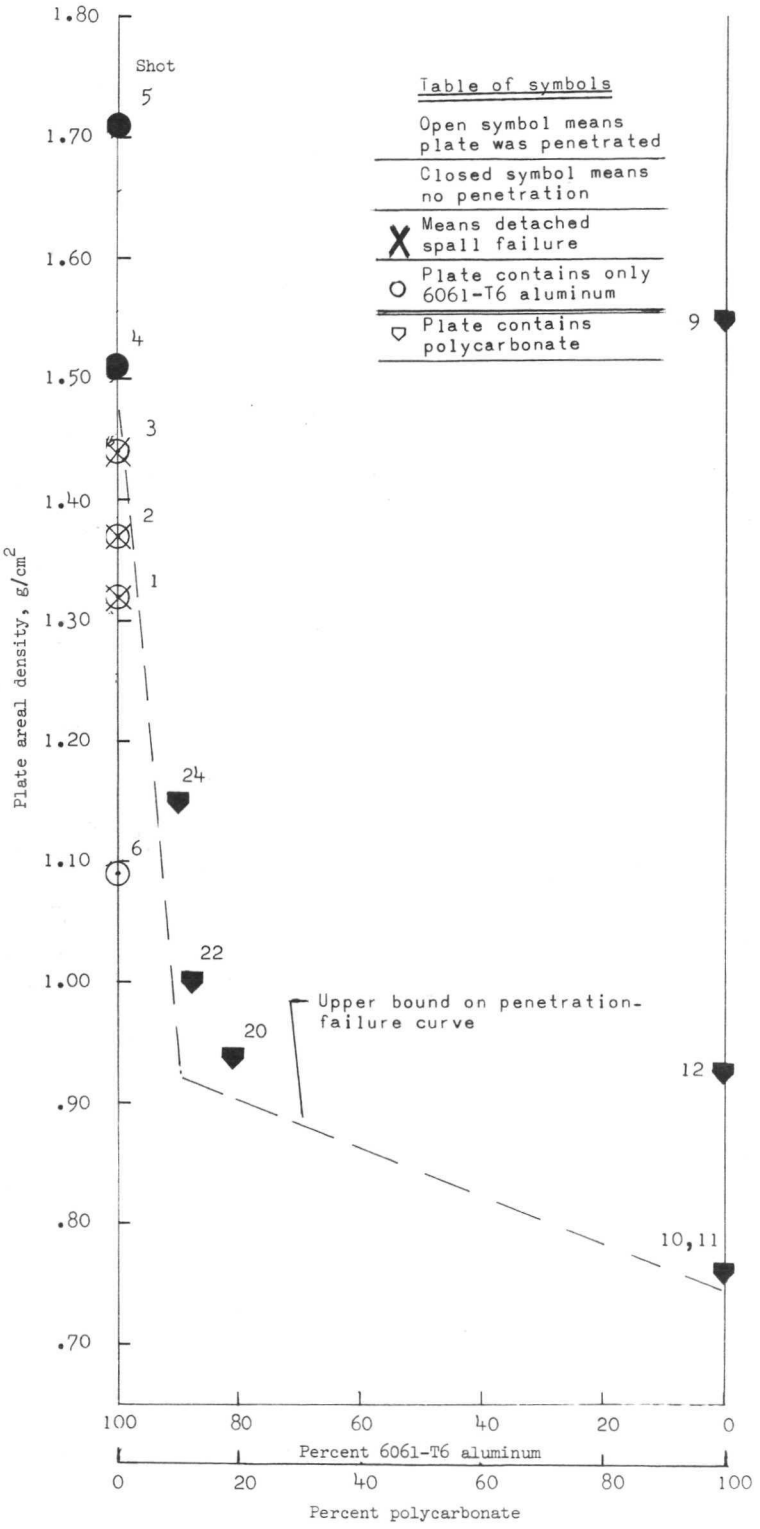

Figure 11.- Percentage from table II of 6061-T6 aluminum and polycarbonate in various plates impacted in the velocity range of 6.25 to 7.25 km/sec.

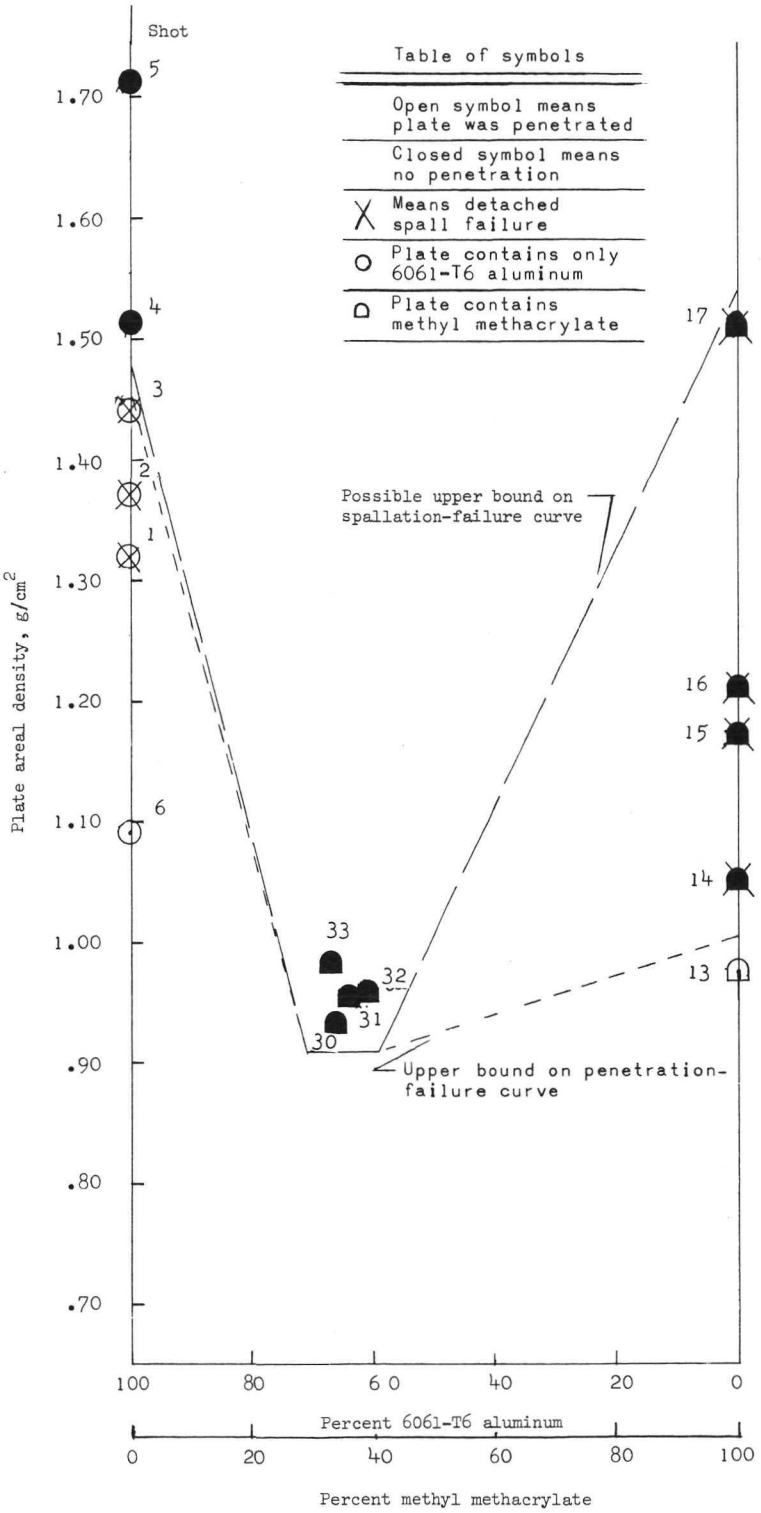

Figure 12.- Percentage from table II of 6061-T6 aluminum and methyl methacrylate in various plates impacted in the velocity range of 6.25 to 7.25 km/sec.

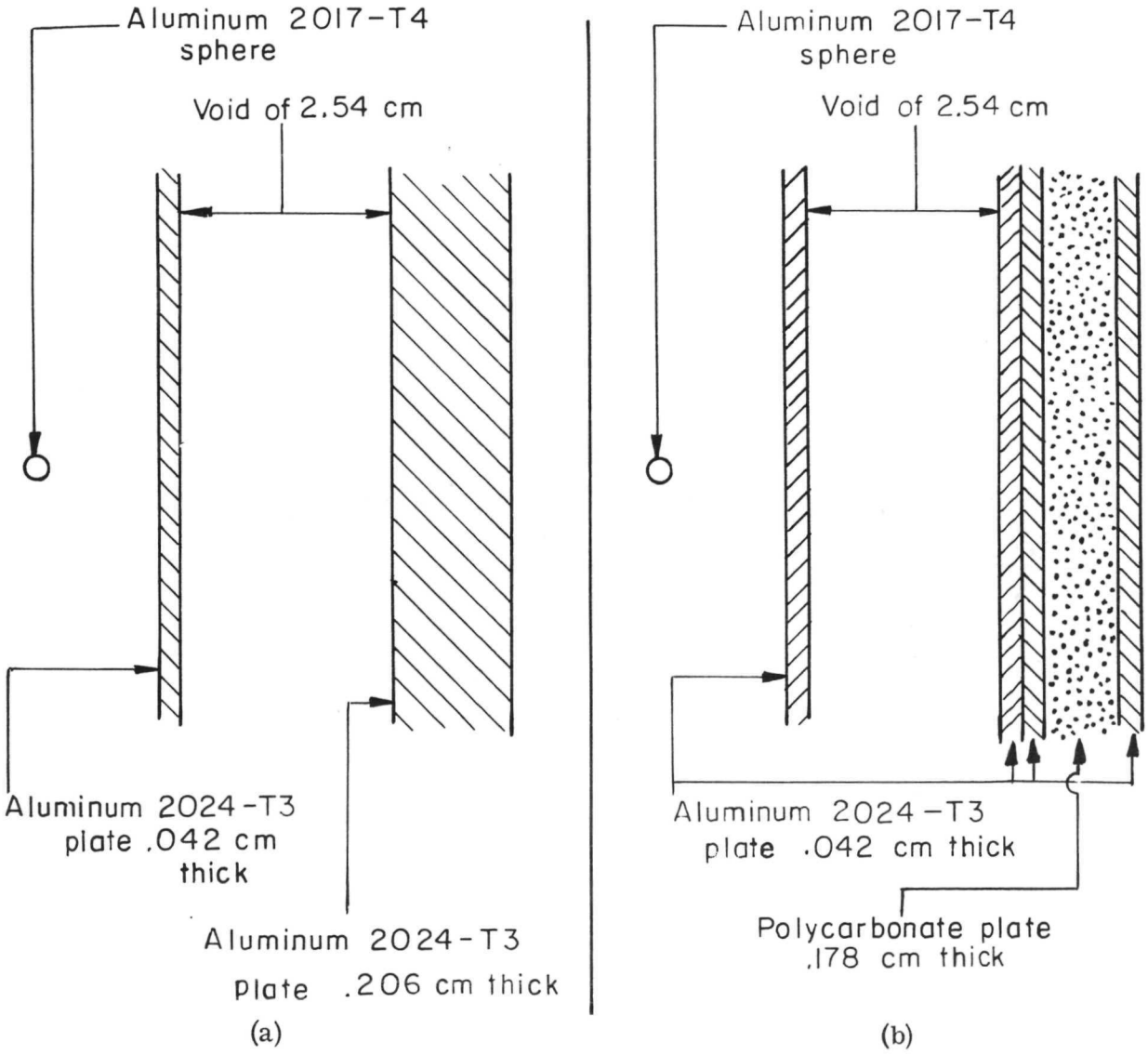

Figure 13.- Schematic of bumper-protected targets.

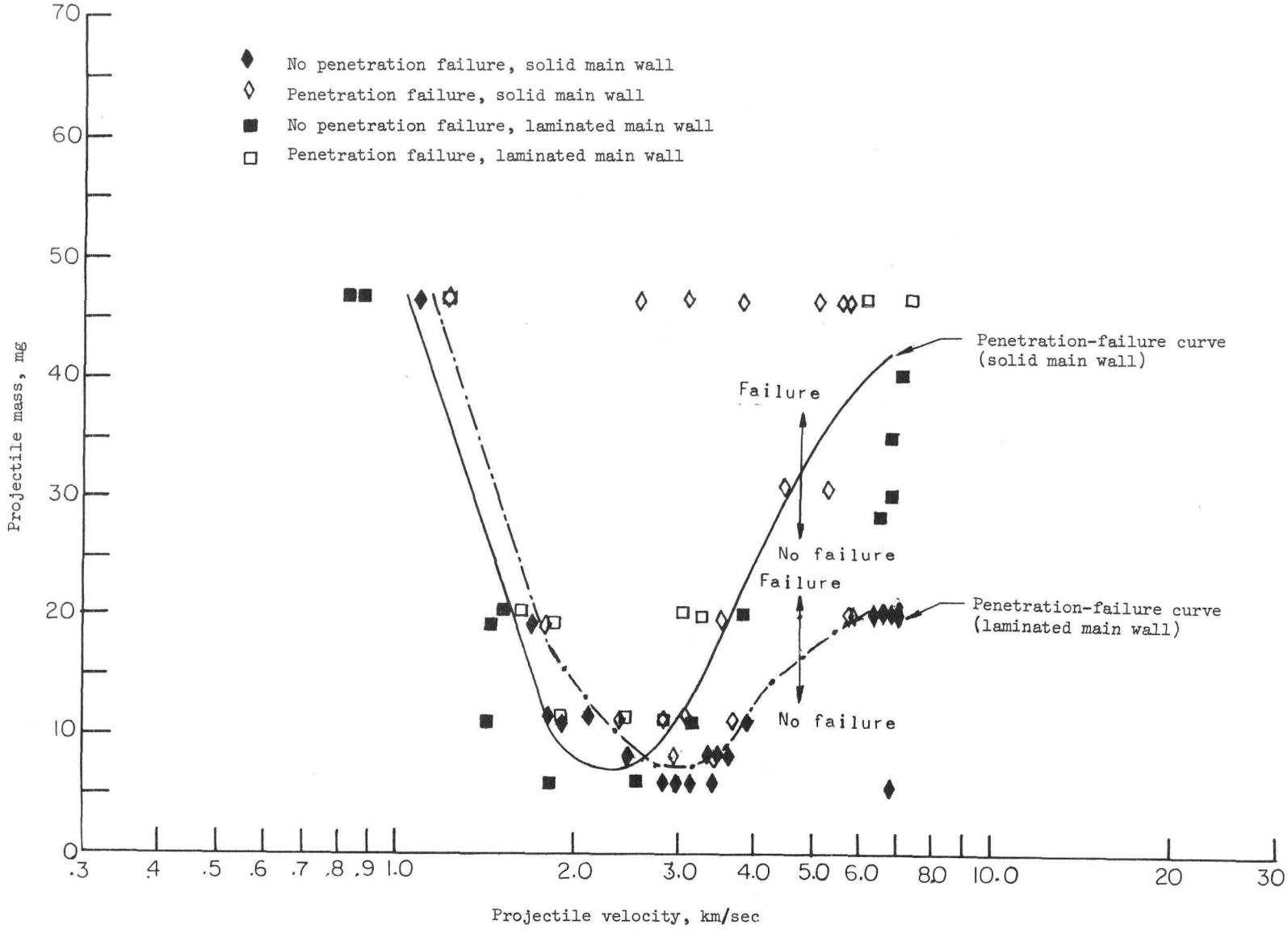

Figure 14.- Plotted data from table III showing penetration-failure curves for laminated and solid main walls.

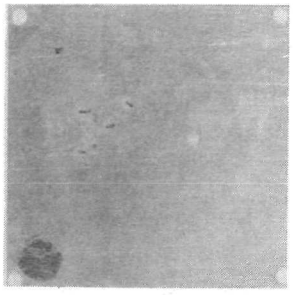

(a) Front view of 2024-T3 aluminum bumper.

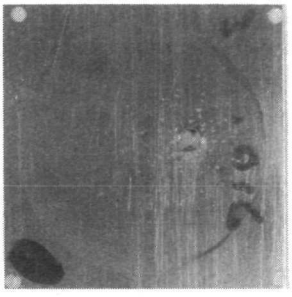

(b) Front view of first 2024-T3 aluminum lamina.

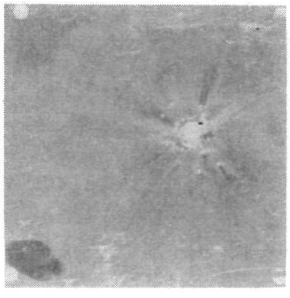

(c) Front view of second 2024-T3 aluminum lamina.

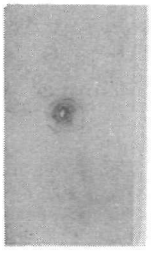

(d) Front view of polycarbonate lamina.

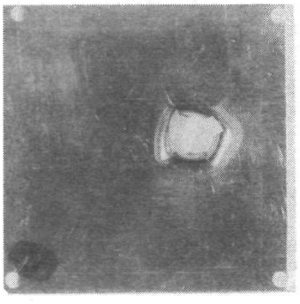

(e) Front view of last 2024-T3 aluminum lamina.

L-72-6568

Figure 15.- Photographs of damage done to a bumper-protected and laminated main wall used in shot 52, table III.

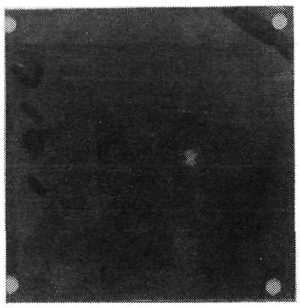

(a) Front view of 2024-T3 aluminum bumper.

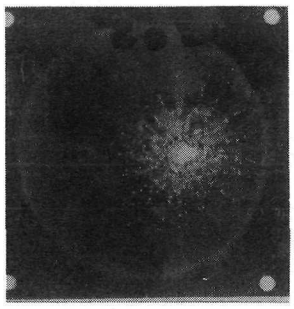

(b) Front view of first 2024-T3 aluminum lamina.

(c) Front view of second 2024-T3 aluminum lamina.

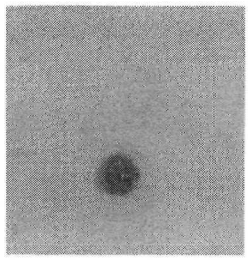

(d) Front view of polycarbonate lamina.

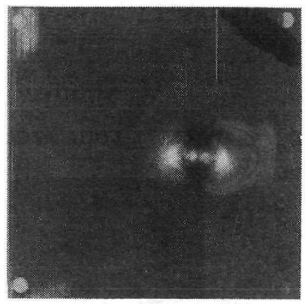

(e) Front view of last 2024-T3 aluminum lamina.

L-72-6569

Figure 16.- Photographs of damage done to a bumper-protected and laminated main wall used in shot 54, table III.

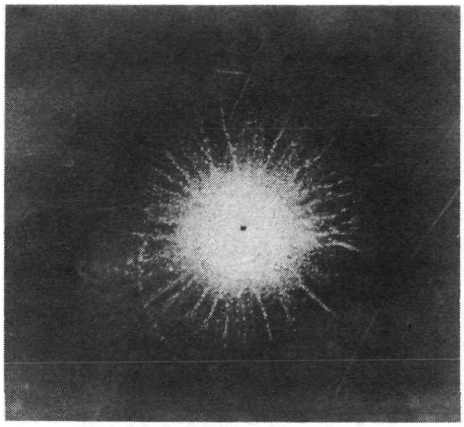

(a) Front view of solid 2024-T3 aluminum main wall.

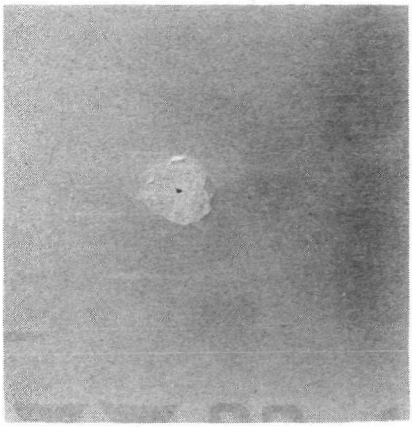

(b) Rear view of solid 2024-T3 aluminum main wall.

L-72-6570

Figure 17.- Photographs of damage done to a solid main wall used in shot 30, table III.

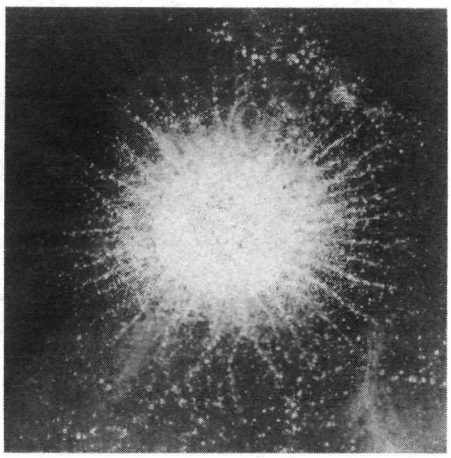

(a) Front view of solid 2024-T3 aluminum main wall.

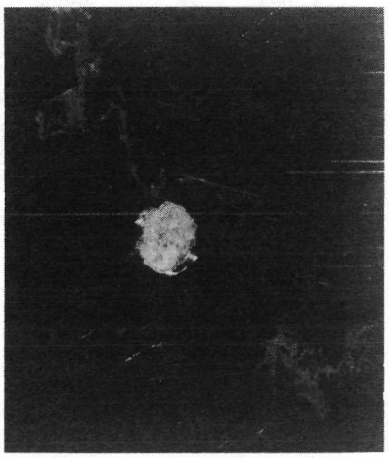

(b) Rear view of solid 2024-T3 aluminum main wall.

L-72-6571

Figure 18.- Photographs of damage done to a solid main wall used in shot 28, table III.

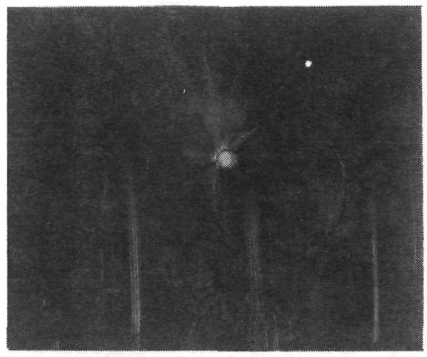

(a) Front view of 2024-T3 aluminum bumper.

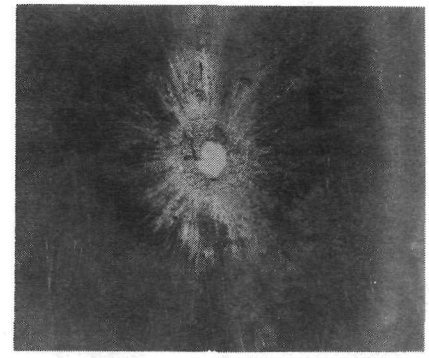

(b) Front view of first 2024-T3 aluminum lamina.

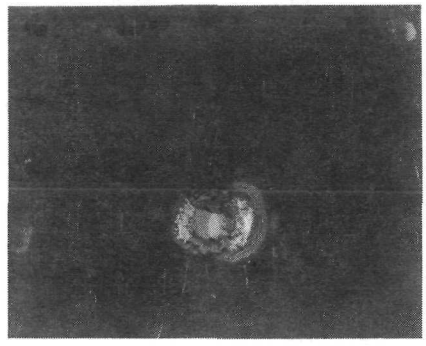

(c) Front view of second 2024-T3 aluminum lamina.

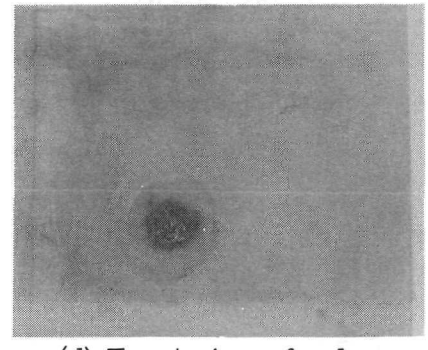

(d) Front view of polycarbonate lamina.

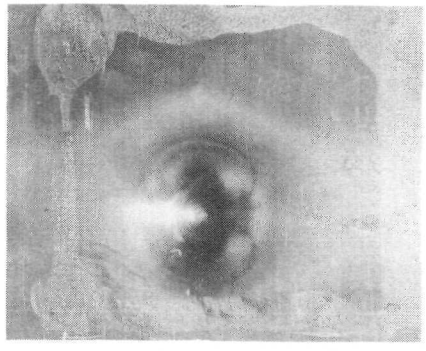

(e) Front view of last 2024-T3 aluminum lamina.

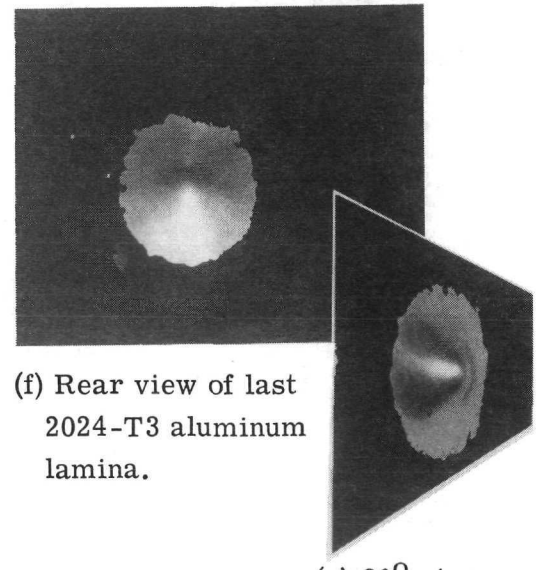

(f) Rear view of last 2024-T3 aluminum lamina.

(g) 30° view from rear of last lamina.

L-72-6572

Figure 19.- Photographs of damage done to a bumper-protected and laminated main wall used in shot 57, table III.

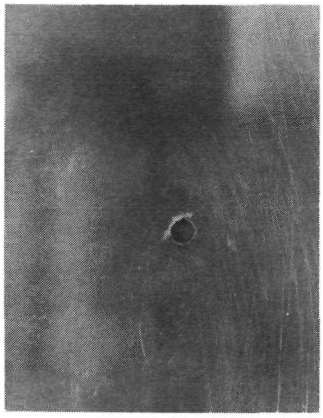

(a) Front view of 2024-T3 aluminum bumper.

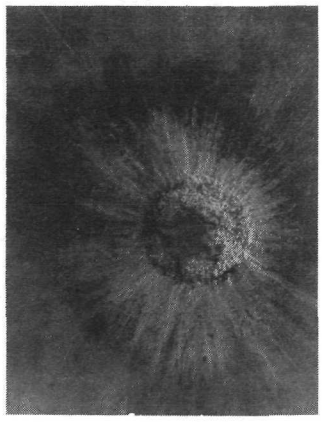

(b) Front view of first and second 2024-T3 aluminum laminae which became welded together during the shot.

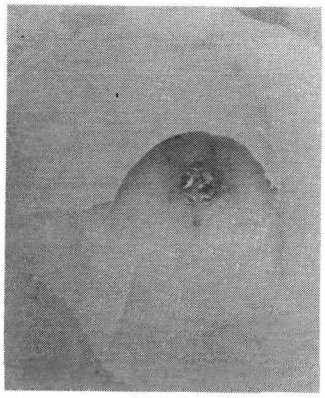

(c) Front view of poly-carbonate lamina.

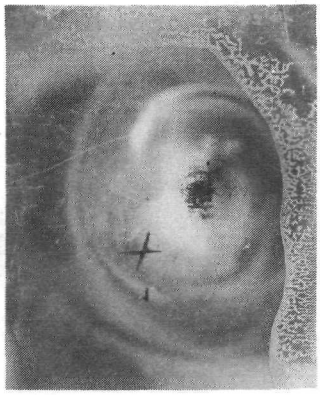

(d) Front view of last 2024-T3 aluminum lamina.

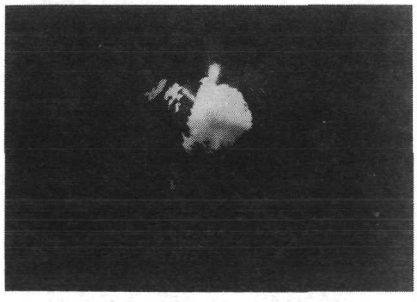

(e) Rear view of last 2024-T3 aluminum lamina.

L-72-6573

Figure 20.- Photographs of damage done to a bumper-protected and laminated main wall used in shot 58, table III.

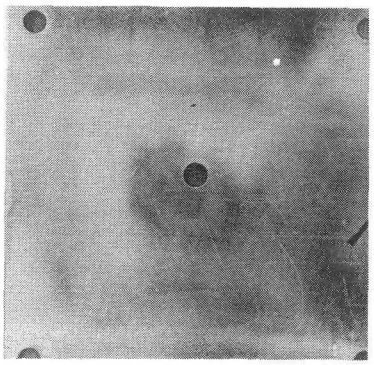

(a) Front view of 2024-T3 aluminum bumper.

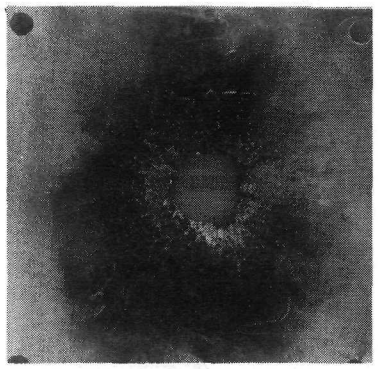

(b) Front view of first 2024-T3 aluminum lamina.

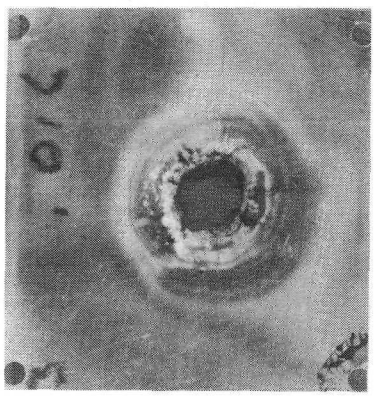

(c) Front view of second 2024-T3 aluminum lamina.

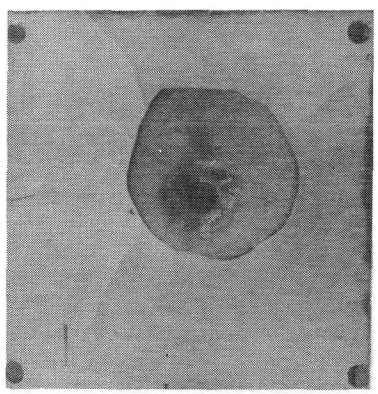

(d) Front view of polycarbonate lamina.

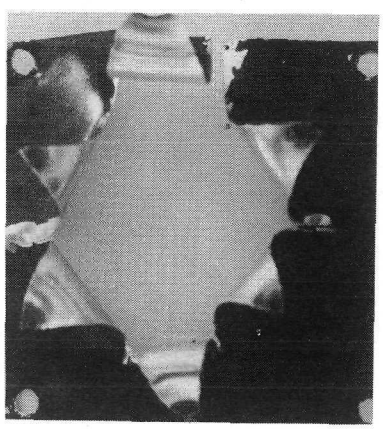

(e) Rear view of last 2024-T3 aluminum lamina.

L-72-6574

Figure 21.- Photographs of damage done to a bumper-protected and laminated main wall used in shot 62, table III.

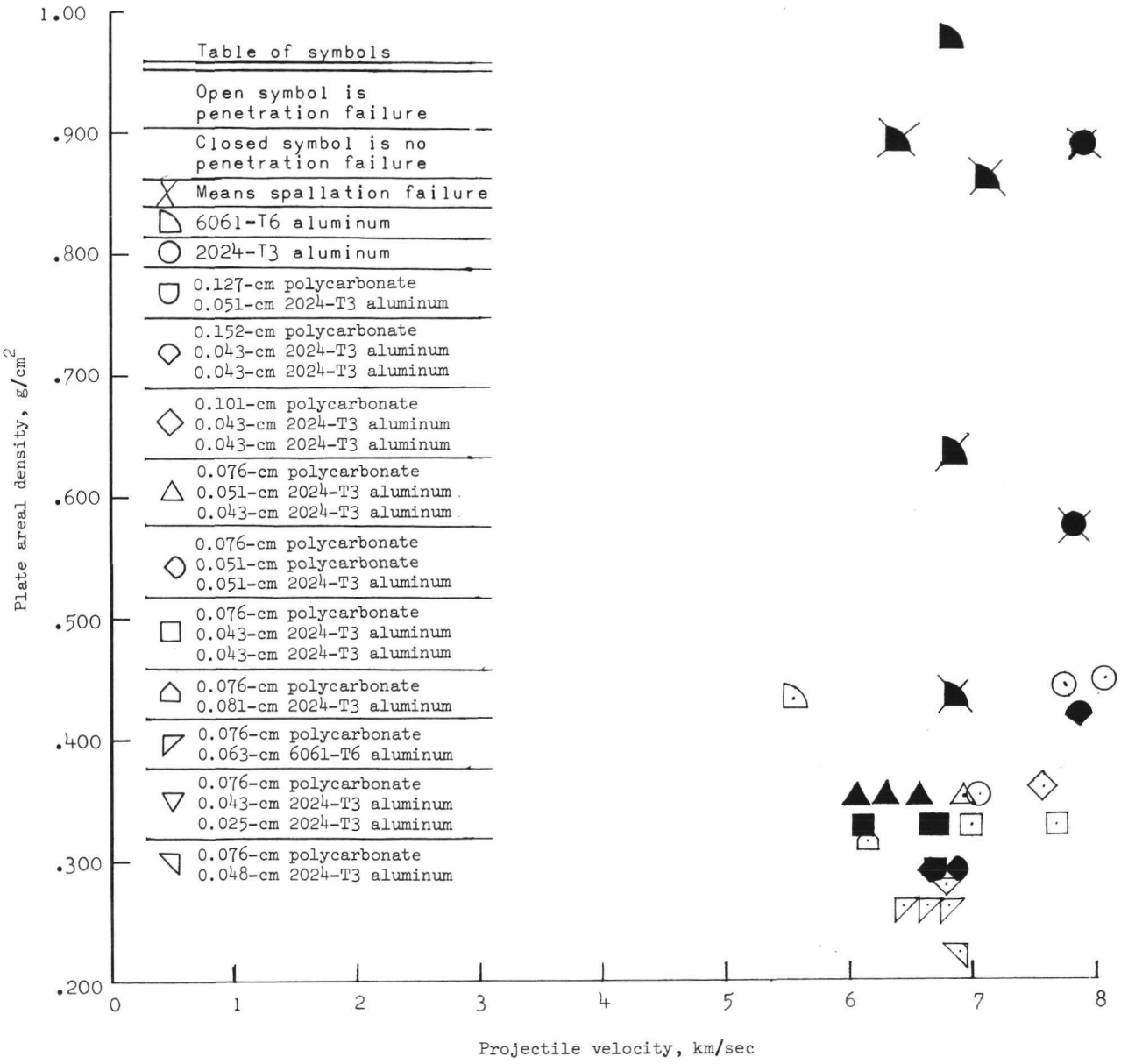

Figure 22.- A comparison of the penetration and spallation resistance of solid aluminum 6061-T6 and 2024-T3 main walls and laminated main walls composed of polycarbonate and either 6061-T6 or 2024-T3 aluminum.

NATIONAL AERONAUTICS AND SPACE ADMINISTRATION
WASHINGTON, D.C. 20546

OFFICIAL BUSINESS
PENALTY FOR PRIVATE USE $300

SPECIAL FOURTH-CLASS RATE BOOK

POSTAGE AND FEES PAID
NATIONAL AERONAUTICS AND SPACE ADMINISTRATION
451

U.S.MAIL

POSTMASTER: If Undeliverable (Section 158 Postal Manual) Do Not Return

"The aeronautical and space activities of the United States shall be conducted so as to contribute . . . to the expansion of human knowledge of phenomena in the atmosphere and space. The Administration shall provide for the widest practicable and appropriate dissemination of information concerning its activities and the results thereof."

—NATIONAL AERONAUTICS AND SPACE ACT OF 1958

NASA SCIENTIFIC AND TECHNICAL PUBLICATIONS

TECHNICAL REPORTS: Scientific and technical information considered important, complete, and a lasting contribution to existing knowledge.

TECHNICAL NOTES: Information less broad in scope but nevertheless of importance as a contribution to existing knowledge.

TECHNICAL MEMORANDUMS: Information receiving limited distribution because of preliminary data, security classification, or other reasons. Also includes conference proceedings with either limited or unlimited distribution.

CONTRACTOR REPORTS: Scientific and technical information generated under a NASA contract or grant and considered an important contribution to existing knowledge.

TECHNICAL TRANSLATIONS: Information published in a foreign language considered to merit NASA distribution in English.

SPECIAL PUBLICATIONS: Information derived from or of value to NASA activities. Publications include final reports of major projects, monographs, data compilations, handbooks, sourcebooks, and special bibliographies.

TECHNOLOGY UTILIZATION PUBLICATIONS: Information on technology used by NASA that may be of particular interest in commercial and other non-aerospace applications. Publications include Tech Briefs, Technology Utilization Reports and Technology Surveys.

Details on the availability of these publications may be obtained from:

SCIENTIFIC AND TECHNICAL INFORMATION OFFICE

NATIONAL AERONAUTICS AND SPACE ADMINISTRATION

Washington, D.C. 20546